Integrated analysis reveals a potential cuproptosis-related ceRNA axis SNHG17/miR-29a-3p/GCSH in prostate adenocarcinoma

Shuyuan Xiao [a], Weiyang Lou [b,*]

[a] Department of Anesthesiology, The First Affiliated Hospital, College of Medicine, Zhejiang University, Hangzhou, China
[b] Department of Breast Surgery, The First Affiliated Hospital, College of Medicine, Zhejiang University, Hangzhou, China

A R T I C L E   I N F O

A B S T R A C T

Cuproptosis is a novel form of programmed cell death. The role and mechanism of cuproptosis-related genes in prostate adenocarcinoma have not been fully understood. In this study, a series of bioinformatic analyses were performed. Consequently, glycine cleavage system protein H with high expression and unfavorable prognosis was regarded as the most potential cuproptosis-related gene in prostate adenocarcinoma. Moreover, glycine cleavage system protein H might be a promising indicator for predicting leuprolide sensitivity in prostate adenocarcinoma and three potential drugs targeting glycine cleavage system protein H were identified. Enrichment analysis revealed that glycine cleavage system protein H-correlated genes were significantly enriched in tricarboxylic acid cycle-related pathways. Subsequently, small nucleolar RNA host gene 17/miR-29a-3p axis was found to partially account for overexpression of glycine cleavage system protein H in prostate adenocarcinoma. Collectively, the current study elucidated a potential cuproptosis-related competing endogenous RNA axis small nucleolar RNA host gene 17/miR-29a-3p/glycine cleavage system protein H in prostate adenocarcinoma.

1. Introduction

Prostate adenocarcinoma is one of the leading causes of cancer-related deaths in men all over the world [1]. Furthermore, approximately 10 % of newly-diagnosed patients with prostate adenocarcinoma present distant metastatic lesions and nearly 5 % patients received surgery eventually develop metastasis [2]. In the past decades, the mechanistic research regarding carcinogenesis and progression of prostate cancer has never stopped, including microRNA (miRNA) [3]. However, despite huge efforts have been put by researchers to study and explore effective therapeutic strategies and drug targets, the survival rate of patients with prostate adenocarcinoma is still not optimistic. Therefore, it would make sense to further explore detailed molecular mechanism responsible for occurrence and development of prostate adenocarcinoma.

As is known to all, insufficient or excessive abundance of heavy metal ions can trigger cell death [4]. As an essential cofactor, copper homeostasis is also important for multiple biological processes. Recently, Tsvetkov et al. proposed a novel form of programmed cell death, namely cuproptosis, that was induced by intracellular copper accumulation and followingly triggered by aggregation of mitochondrial lipoylated proteins of tricarboxylic acid (TCA) cycle [5,6]. Several genes have been identified to be involved in cuproptosis, including SLC31A1, DLAT, ATP7B, FDX1 and LIAS [4]. Recently, the role and mechanism of cuproptosis-related genes in human malignancies have been reported. For example, Bian et al. suggested that cuproptosis-related gene signature could sever as a

---

Abbreviations

AUC	Area Under Curve
CCLE	Cancer Cell Line Encyclopedia
ceRNA	competing endogenous RNA
GCSH	glycine cleavage system protein H
GO	Gene Ontology
KEGG	Kyoto Encyclopedia of Genes and Genomes
miRNA	microRNA
ncRNA	non-coding RNA
ROC	Receiver Operating Characteristic
SNHG17	small nucleolar RNA host gene 17
TCA	tricarboxylic acid
TCGA	The Cancer Genome Atlas

potential prognostic predictor for clear cell renal cell carcinoma [7]. However, a comprehensive study for the expression, mechanism and prognosis of cuproptosis-related genes in prostate adenocarcinoma is still absent and deserves to be conducted.

In this study, the expression levels of cuproptosis-related genes in prostate adenocarcinoma were firstly analyzed and validated. Next, the prognostic values of potential cuproptosis-related genes in prostate adenocarcinoma were assessed. Subsequently, the downstream action mechanism and upstream non-coding RNA (ncRNA) regulatory mechanism of GCSH in prostate adenocarcinoma were explored. The current findings from this study elucidated a potential cuproptosis-related competing endogenous RNA (ceRNA) axis SNHG17/miR-29a-3p/GCSH in prostate adenocarcinoma.

2. Results

2.1. The expression levels of cuproptosis-related genes in prostate adenocarcinoma

By reviewing publications, a total of 19 cuproptosis-related genes, involving NFE2L2, NLRP3, ATP7B, ATP7A, SLC31A1, FDX1, LIAS, LIPT1, LIPT2, DLD, DLAT, PDHA1, PDHB, MTF1, GLS, CDKN2A, DBT, GCSH and DLST, were included for subsequent analysis. To explore the potential roles of cuproptosis-related genes in prostate adenocarcinoma, the expression levels of these genes were determined using starBase and GEPIA databases. As shown in Table 1, many of them were aberrantly expressed in prostate adenocarcinoma. However, only five cuproptosis-related genes, consisting of NFE2L2 (downregulated), ATP7B (upregulated), CDKN2A (upregulated), GCSH (upregulated) and DLST (downregulated), were commonly markedly dysregulated in prostate adenocarcinoma when compared with corresponding normal controls in both the above two databases. The expression levels of them were vividly presented in Fig. 1A–J. These results indicated that the five cuproptosis-related genes may be key regulators in initiation and progression of prostate adenocarcinoma.

Table 1

The expression levels of cuproptosis-related genes in prostate adenocarcinoma determined by starBase and GEPIA databases.

| Gene	Cancer Exp	Normal Exp	FC	$\log_2$FC	P-value	starBase	GEPIA
NFE2L2	15.15	22.91	0.66	−0.60	1.40E-15	down	down
NLRP3	0.52	0.71	0.73	−0.45	1.60E-02	down	no
ATP7B	3.39	2.15	1.57	0.65	4.30E-06	up	up
ATP7A	3.49	3.66	0.95	−0.07	2.10E-01	no	up
SLC31A1	17.80	21.71	0.82	−0.29	2.00E-03	down	up
FDX1	7.87	12.90	0.61	−0.71	3.20E-05	down	up
LIAS	3.54	3.68	0.96	−0.06	1.80E-01	no	no
LIPT1	3.56	3.22	1.11	0.15	1.20E-01	no	down
LIPT2	1.71	1.58	1.08	0.11	5.90E-02	no	up
DLD	14.79	15.59	0.95	−0.07	5.50E-02	no	up
DLAT	8.06	8.58	0.94	−0.09	4.50E-02	down	up
PDHA1	12.50	12.82	0.97	−0.04	6.50E-01	no	down
PDHB	13.93	13.51	1.03	0.04	4.20E-01	no	up
MTF1	2.63	2.69	0.98	−0.03	4.40E-01	no	no
GLS	4.64	4.95	0.94	−0.09	7.30E-02	no	down
CDKN2A	0.92	0.39	2.38	1.25	3.80E-15	up	up
DBT	5.76	5.76	1.00	0.00	6.10E-01	no	up
GCSH	2.97	2.60	1.14	0.19	2.80E-02	up	up
DLST	20.16	21.46	0.94	−0.09	2.90E-02	down	down
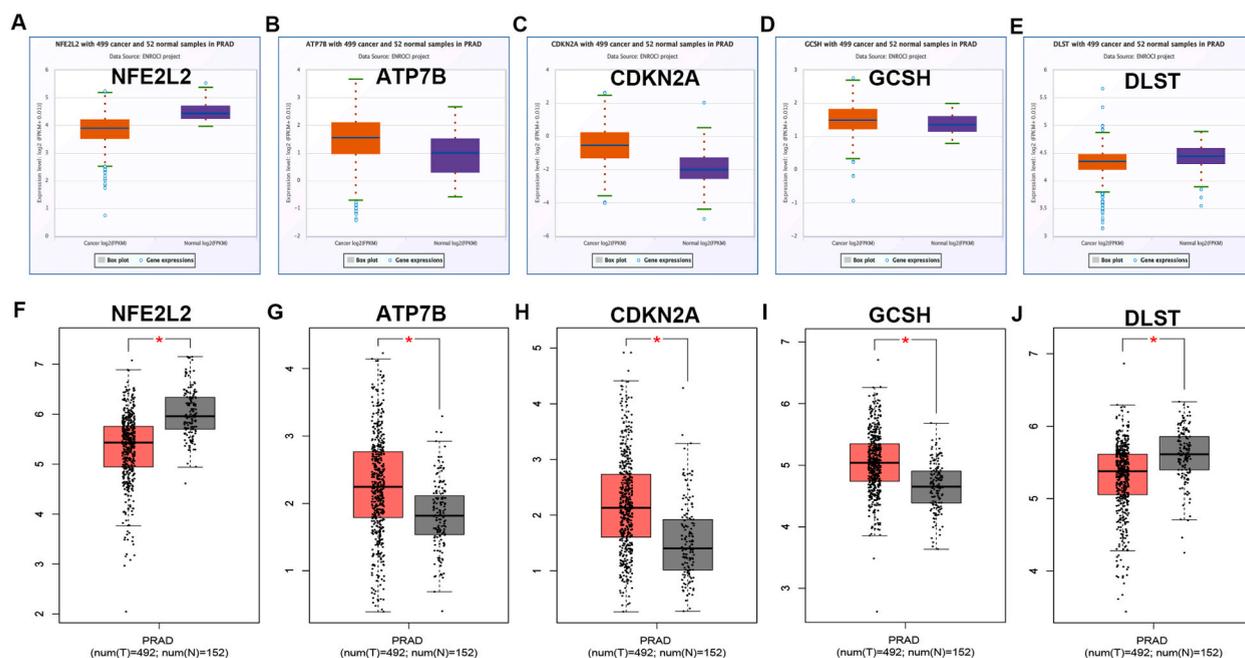
Fig. 1. Expression analysis for cuproptosis-related genes in prostate adenocarcinoma. The expression levels of five cuproptosis-related genes NFE2L2 (A), ATP7B (B), CDKN2A (C), GCSH (D) and DLST (E) in prostate adenocarcinoma and normal controls (only TCGA normal tissues) analyzed by starBase database. The expression levels of five cuproptosis-related genes NFE2L2 (F), ATP7B (G), CDKN2A (H), GCSH (I) and DLST (J) in prostate adenocarcinoma and normal controls (contain TCGA normal tissues and GTEx normal samples) analyzed by GEPIA database. *$P < 0.05$.

2.2. The prognostic values of cuproptosis-related genes in prostate adenocarcinoma

Next, survival analysis for NFE2L2, ATP7B, CDKN2A, GCSH or DLST was performed by usage of The Cancer Genome Atlas (TCGA) prostate adenocarcinoma expression and survival data. As presented in Fig. 2A–E, among the five genes, only prostate adenocarcinoma patients with higher expression of GCSH possessed poorer prognosis (P-value equal to 0.038). The data from Cancer Cell Line Encyclopedia (CCLE) database also showed presence of GCSH in prostate cancer cell lines (Table S1). For the other cuproptosis-related genes, no statistical significance of them in predicting prognosis of prostate adenocarcinoma was observed. Taken high expression of GCSH and its unfavorable prognostic value into consideration, GCSH might be the most potential cuproptosis-related gene in prostate adenocarcinoma.

2.3. Enrichment analysis for GCSH-correlated genes

In order to better understand molecular action mechanism of GCSH, its correlated genes with combined scores more than 0.4 were firstly obtained using STRING database. For better visualization, a GCSH-correlated gene network was established as shown in Fig. 3A. Next, Gene Ontology (GO) functional annotation and pathway enrichment analysis were conducted for these GCSH-related genes. As presented in Fig. 3B-D, these GCSH-related genes were significantly enriched in glycine decarboxylation *via* glycine cleavage system and cellular response to tetrahydrofolate in GO biological process category, glycine cleavage complex and oxoglutarate dehydrogenase complex in GO cellular component category, and L-allo-threonine aldolase activity, glycine hydroxymethyltransferase activity and aminomethyltransferase activity in GO molecular function category. For pathway enrichment analysis, two databases were included, consisting of Kyoto Encyclopedia of Genes and Genomes (KEGG) and Wiki. The top two enriched pathways were lipoic acid metabolism and glyoxylate and dicarboxylate metabolism in KEGG, and glycine metabolism and serine metabolism in Wiki (Fig. 3E and F). Moreover, for further exploring molecular mechanism, the genes that were significantly correlated with GCSH were also identified by three other databases, including cBioPortal, UALCAN and GEPIA (Table S2). By performing intersection analysis, a total of 30 genes were commonly appeared in all the three databases as shown in Fig. 3G, which might be the most potential genes linked to GCSH.

2.4. Identification of potential GCSH-related drugs in prostate adenocarcinoma

Leuprolide, a gonadotropin releasing hormone agonist, is widely used predominantly to manage and treat prostate cancer [8]. To study the potential role of GCSH in predicting therapeutic sensitivity of leuprolide in prostate adenocarcinoma, CTR-DB database was employed. As shown in Fig. 4A, the expression of GCSH was markedly increased in leuprolide-treated response group when compared with non-response group in prostate adenocarcinoma. Receiver Operating Characteristic (ROC) curve analysis revealed that GCSH possessed statistical significance to distinguish response group from non-response group after treatment of leuprolide in prostate
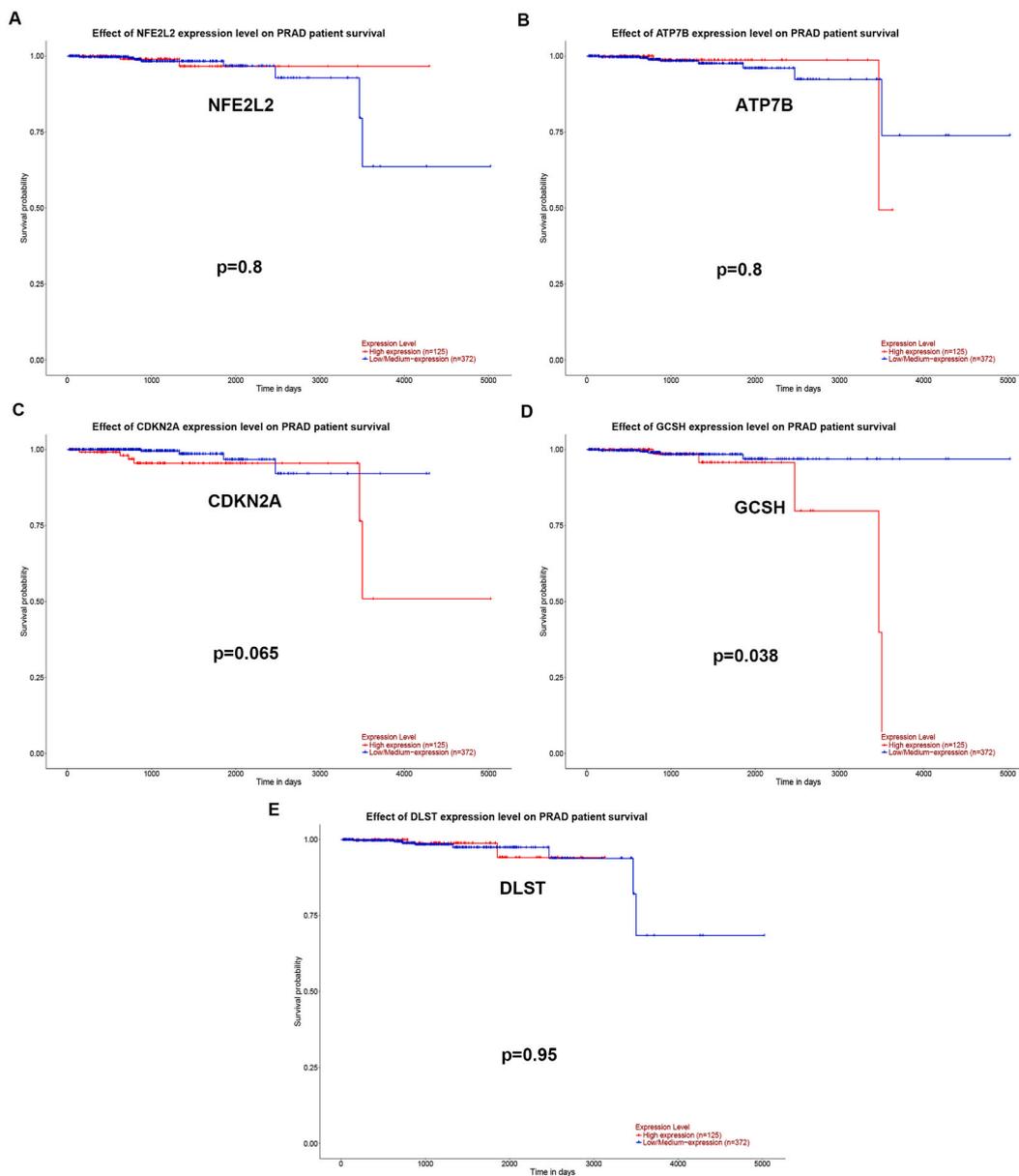
Fig. 2. Survival analysis for five cuproptosis-related genes in prostate adenocarcinoma using UALCAN database. The prognostic values of NFE2L2 (A), ATP7B (B), CDKN2A (C), GCSH (D) and DLST (E) in prostate adenocarcinoma.

adenocarcinoma, with its Area Under Curve (AUC) value equal to 0.811 (Fig. 4B). Furthermore, to explore other possible drugs targeting GCSH in prostate adenocarcinoma, TISIDB database was introduced. As suggested in Fig. 4C, three small molecule drugs targeting GCSH were obtained, consisting of DB00145, DB03187 and DB03760.

2.5. The potential upstream miRNAs of GCSH in prostate adenocarcinoma

To uncover miRNA regulation mechanism, the upstream miRNAs of GCSH were predicted using online target gene prediction tools. Consequently, 47 miRNAs that might potentially bind to GCSH were obtained (Fig. 5A). Correlation analysis was subsequently performed using TCGA prostate adenocarcinoma data (Table 2). As shown in Fig. 5B and 19 of 47 miRNAs (40.4 %) were significantly negatively correlated with GCSH in prostate adenocarcinoma. Next, the expression levels of the 19 miRNAs in prostate adenocarcinoma were determined by starBase database (Fig. 5C). Among the 19 miRNAs, only 4 miRNAs were markedly downregulated in prostate adenocarcinoma when compared with normal control, consisting of miR-212–3p, miR-29a-3p, miR-410–3p and miR-144–3p. UALCAN database was also employed to analyze the 4 miRNAs' expression in prostate adenocarcinoma. As presented in Fig. 5D–G,
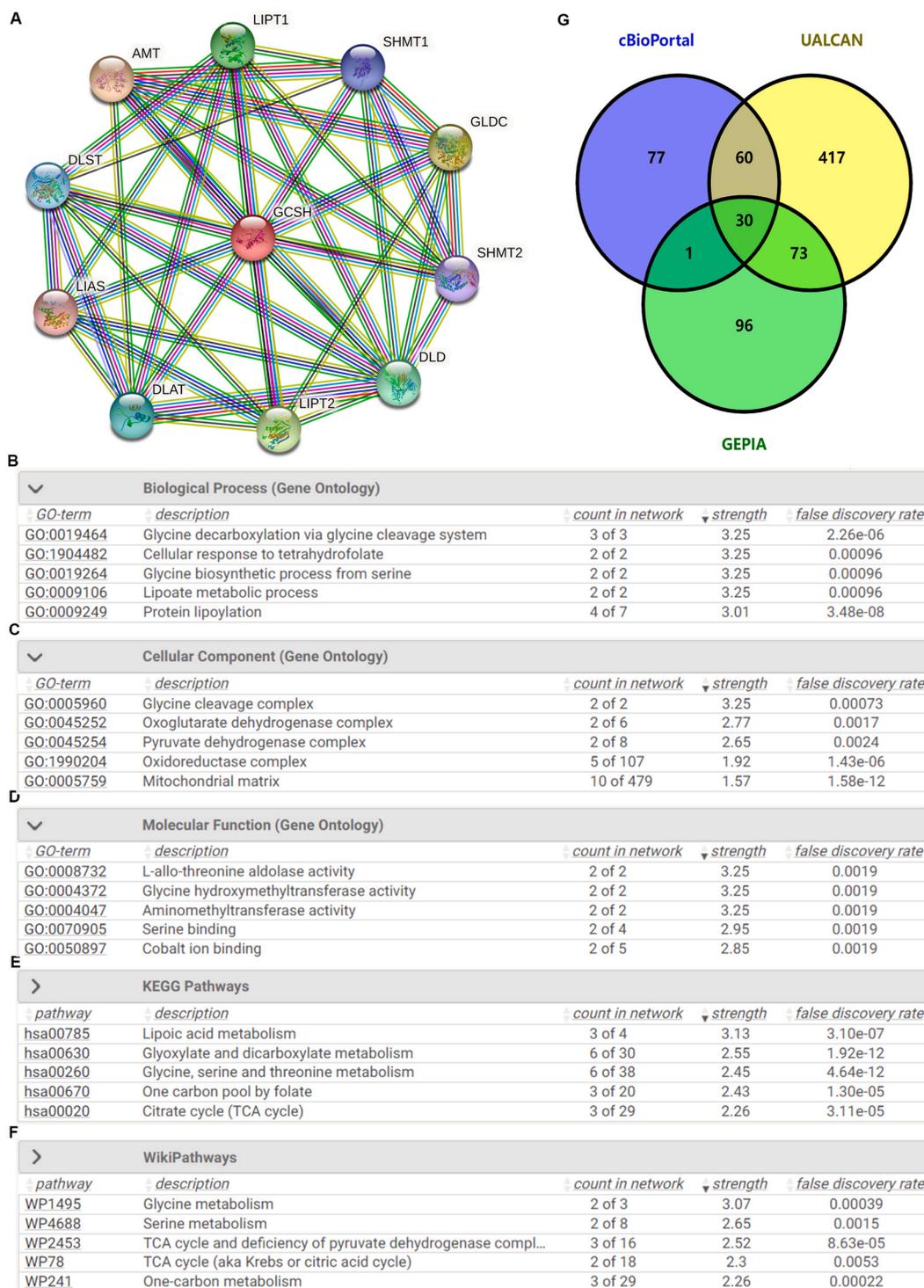
Fig. 3. Enrichment analysis for these genes correlated with GCSH. (A) The protein-protein interaction network of GCSH. The top five enriched Gene Ontology biological process items (B), Gene Ontology cellular component items (C), Gene Ontology molecular function items (D), Kyoto Encyclopedia of Genes and Genomes pathways (E) and Wiki pathways (F) for the GCSH-correlated genes. (G) The intersection analysis for the GCSH-correlated genes from cBioPortal, UALCAN and GEPIA databases.

B

Biological Process (Gene Ontology)				
GO-term	description	count in network	strength	false discovery rate
GO:0019464	Glycine decarboxylation via glycine cleavage system	3 of 3	3.25	2.26e-06
GO:1904482	Cellular response to tetrahydrofolate	2 of 2	3.25	0.00096
GO:0019264	Glycine biosynthetic process from serine	2 of 2	3.25	0.00096
GO:0009106	Lipoate metabolic process	2 of 2	3.25	0.00096
GO:0009249	Protein lipoylation	4 of 7	3.01	3.48e-08

C

Cellular Component (Gene Ontology)				
GO-term	description	count in network	strength	false discovery rate
GO:0005960	Glycine cleavage complex	2 of 2	3.25	0.00073
GO:0045252	Oxoglutarate dehydrogenase complex	2 of 6	2.77	0.0017
GO:0045254	Pyruvate dehydrogenase complex	2 of 8	2.65	0.0024
GO:1990204	Oxidoreductase complex	5 of 107	1.92	1.43e-06
GO:0005759	Mitochondrial matrix	10 of 479	1.57	1.58e-12

D

Molecular Function (Gene Ontology)				
GO-term	description	count in network	strength	false discovery rate
GO:0008732	L-allo-threonine aldolase activity	2 of 2	3.25	0.0019
GO:0004372	Glycine hydroxymethyltransferase activity	2 of 2	3.25	0.0019
GO:0004047	Aminomethyltransferase activity	2 of 2	3.25	0.0019
GO:0070905	Serine binding	2 of 4	2.95	0.0019
GO:0050897	Cobalt ion binding	2 of 5	2.85	0.0019

E

KEGG Pathways				
pathway	description	count in network	strength	false discovery rate
hsa00785	Lipoic acid metabolism	3 of 4	3.13	3.10e-07
hsa00630	Glyoxylate and dicarboxylate metabolism	6 of 30	2.55	1.92e-12
hsa00260	Glycine, serine and threonine metabolism	6 of 38	2.45	4.64e-12
hsa00670	One carbon pool by folate	3 of 20	2.43	1.30e-05
hsa00020	Citrate cycle (TCA cycle)	3 of 29	2.26	3.11e-05

F

WikiPathways				
pathway	description	count in network	strength	false discovery rate
WP1495	Glycine metabolism	2 of 3	3.07	0.00039
WP4688	Serine metabolism	2 of 8	2.65	0.0015
WP2453	TCA cycle and deficiency of pyruvate dehydrogenase compl...	3 of 16	2.52	8.63e-05
WP78	TCA cycle (aka Krebs or citric acid cycle)	2 of 18	2.3	0.0053
WP241	One-carbon metabolism	3 of 29	2.26	0.00022

Fig. 4. The relationship of GCSH expression with drug response to leuprolide treatment and potential drugs targeting GCSH in prostate adenocarcinoma. (A) The expression levels of GCSH in non-response group and response group after treatment of leuprolide in prostate adenocarcinoma. (B) The role of GCSH in predicting therapeutic sensitivity of leuprolide in prostate adenocarcinoma (AUC curve). (C) The potential drugs targeting GCSH obtained from TISIDB database.

miR-212–3p, miR-29a-3p and miR-410–3p were markedly downregulated in prostate adenocarcinoma but no statistical expression difference of miR-144–3p between prostate adenocarcinoma tissues and normal tissues was observed. Correlation analysis revealed that all the four miRNAs were significantly inversely correlated with GCSH in prostate cancer (Fig. S1). CancerMIRNome database analysis indicated that all the four miRNAs were significantly downregulated (Fig. 5H–K) and possessed statistical diagnostic values (Fig. 5L-O, miR-212–3p (AUC = 0.80), miR-29a-3p (AUC = 0.76), miR-410–3p (AUC = 0.78), miR-144–3p (AUC = 0.73)) in prostate adenocarcinoma. The potential upstream miRNAs of GCSH should be tumor suppressive miRNAs in prostate adenocarcinoma. However, previous studies reported the oncogenic role of miR-410–3p in prostate adenocarcinoma [9]. Taken together, miR-212–3p and miR-29a-3p might be the most potential upstream miRNAs of GCSH in prostate adenocarcinoma.

2.6. The potential upstream lncRNAs of miR-212–3p/miR-29a-3p-GCSH axis in prostate adenocarcinoma

It has been widely acknowledged that lncRNA could sponge with miRNA and then release its suppression of downstream target gene expression and function [10–12]. Therefore, the upstream binding lncRNAs of miR-212–3p or miR-29a-3p were predicted, and consequently 66 and 144 possible lncRNAs of miR-212–3p and miR-29a-3p were obtained, respectively. Subsequently, correlation analysis was performed. As shown in Table S3, Table 3 and Fig. 6A and B, 20 of 66 lncRNAs (30.3 %) were significantly negatively correlated with miR-212–3p, and 8 of the 20 (40 %) lncRNAs were markedly positively associated with GCSH in prostate adenocarcinoma. The expression levels of the 8 lncRNAs were further determined using starBase database. Among the 8 lncRNAs, only AC012640.2, AL391244.1 and AL603839.3 were significantly upregulated in prostate adenocarcinoma tissues when compared with normal controls (Fig. 6C-D). No statistical prognostic values of AC012640.2, AL391244.1, AC092803.2 and AL603839.3 in prostate adenocarcinoma were observed (Fig. 6E–H). As presented in Table S4, Table 3 and Fig. 7A and B, 27 of 114 lncRNAs (23.7 %) were
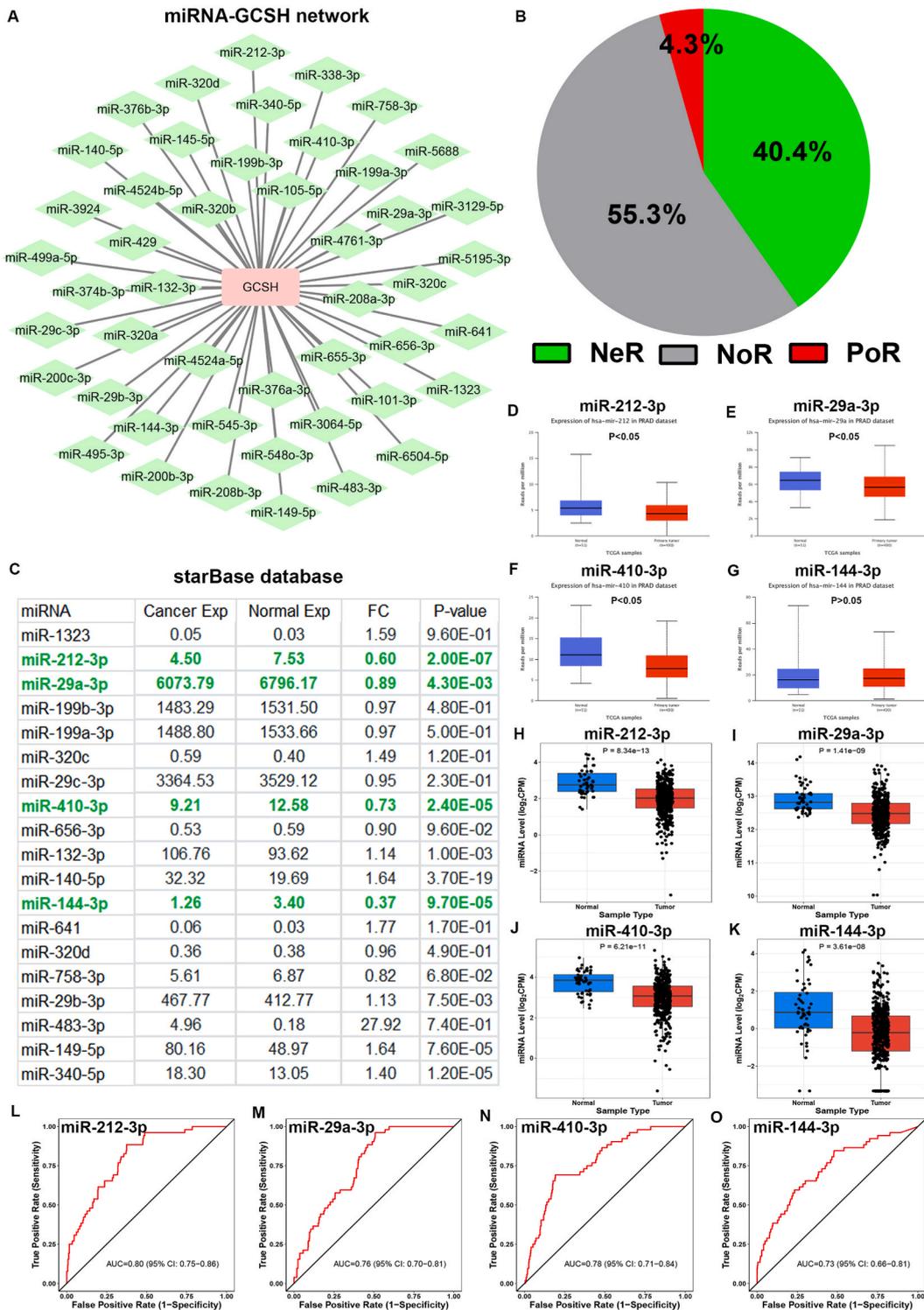
Fig. 5. Prediction and analysis of upstream miRNAs of GCSH in prostate adenocarcinoma. (A) The miRNA-GCSH network established by Cytoscape software. (B) The pie chart of expression correlation of GCSH with its predicted miRNAs in prostate adenocarcinoma analyzed by starBase database. (C) The expression landscape of the miRNAs negatively correlated with GCSH in prostate adenocarcinoma determined by starBase database. The expression levels of miR-212–3p (D), miR-29a-3p (E), miR-410–3p (F) and miR-144–3p (G) in prostate adenocarcinoma and normal controls analyzed by UALCAN database. The expression levels of miR-212–3p (H), miR-29a-3p (I), miR-410–3p (J) and miR-144–3p (K) in prostate adenocarcinoma and normal controls analyzed by CancerMIRNome database. The diagnostic values of miR-212–3p (L), miR-29a-3p (M), miR-410–3p (N) and miR-144–3p (O) in prostate adenocarcinoma evaluated by CancerMIRNome database.

Table 2

The expression correlation of GCSH and its predicted miRNAs in prostate adenocarcinoma analyzed by starBase database.

miRNA	Gene	R-value	P-value
miR-1323	**GCSH**	**−0.202**	**6.10E-06**
miR-212-3p	**GCSH**	**−0.185**	**3.45E-05**
miR-29a-3p	**GCSH**	**−0.184**	**3.90E-05**
miR-199b-3p	**GCSH**	**−0.168**	**1.81E-04**
miR-199a-3p	**GCSH**	**−0.167**	**1.93E-04**
miR-320c	**GCSH**	**−0.156**	**5.09E-04**
miR-29c-3p	**GCSH**	**−0.154**	**5.66E-04**
miR-410-3p	**GCSH**	**−0.154**	**5.70E-04**
miR-656-3p	**GCSH**	**−0.147**	**1.01E-03**
miR-132-3p	**GCSH**	**−0.125**	**5.34E-03**
miR-140-5p	**GCSH**	**−0.110**	**1.46E-02**
miR-144-3p	**GCSH**	**−0.110**	**1.44E-02**
miR-641	**GCSH**	**−0.101**	**2.47E-02**
miR-320d	**GCSH**	**−0.100**	**2.61E-02**
miR-758-3p	**GCSH**	**−0.097**	**3.07E-02**
miR-29b-3p	**GCSH**	**−0.095**	**3.45E-02**
miR-483-3p	**GCSH**	**−0.093**	**3.94E-02**
miR-149-5p	**GCSH**	**−0.091**	**4.19E-02**
miR-340-5p	**GCSH**	**−0.091**	**4.36E-02**
miR-320 b	GCSH	−0.069	1.27E-01
miR-6504–5p	GCSH	−0.068	1.32E-01
miR-145–5p	GCSH	−0.067	1.37E-01
miR-655–3p	GCSH	−0.067	1.39E-01
miR-499a-5p	GCSH	−0.065	1.46E-01
miR-208 b-3p	GCSH	−0.050	2.67E-01
miR-3064–5p	GCSH	−0.049	2.76E-01
miR-376 b-3p	GCSH	−0.047	2.93E-01
miR-101–3p	GCSH	−0.045	3.23E-01
miR-548o-3p	GCSH	−0.032	4.77E-01
miR-376a-3p	GCSH	−0.020	6.65E-01
miR-4524a-5p	GCSH	−0.020	6.53E-01
miR-495–3p	GCSH	−0.018	6.95E-01
miR-374 b-3p	GCSH	−0.014	7.56E-01
miR-545–3p	GCSH	−0.010	8.26E-01
miR-208a-3p	GCSH	−0.009	8.37E-01
miR-3129–5p	GCSH	−0.002	9.63E-01
miR-105–5p	GCSH	−0.001	9.81E-01
miR-3924	GCSH	0.000	1.00 E+00
miR-5195–3p	GCSH	0.000	1.00 E+00
miR-4524 b-5p	GCSH	0.000	1.00 E+00
miR-4761–3p	GCSH	0.014	7.49E-01
miR-200 b-3p	GCSH	0.023	6.04E-01
miR-338–3p	GCSH	0.045	3.18E-01
miR-429	GCSH	0.051	2.57E-01
miR-320a	GCSH	0.059	1.88E-01
miR-5688	GCSH	0.099	2.80E-02
miR-200c-3p	GCSH	0.215	1.36E-06

The bold values indicate that these results are statistically significant (Negative correlation).

significantly negatively correlated with miR-29a-3p, and 15 of the 27 (55.6 %) lncRNAs were markedly positively associated with GCSH in prostate adenocarcinoma. Expression analysis revealed that 10 of the 15 lncRNAs were obviously upregulated in prostate adenocarcinoma (Fig. 7D), among which only high expression of SNHG17 indicated unfavorable prognosis of prostate adenocarcinoma (Fig. 7E). Based on ceRNA mechanism, by combination of the results from expression analysis, correlation analysis and survival analysis, a potential cuproptosis-related ceRNA axis SNHG17/miR-29a-3p/GCSH in prostate adenocarcinoma was established as shown in Fig. 8.

3. Discussion

Cuproptosis, a novel form of programmed cell death, has come into researchers' eyes. A recent study reported the critical role of cuproptosis-related genes in human clear cell renal cell carcinoma [7]. However, its specific role and mechanism of cuproptosis-related genes in prostate adenocarcinoma are still unknown and need to be further explored.

In this study, by reviewing literatures, a total of 19 cuproptosis-related genes were included. By performing expression analysis and survival analysis, the most potential overexpressed cuproptosis-related gene GCSH in prostate adenocarcinoma was identified. Previous studies have confirmed that GCSH functions as an oncogene in several human malignancies, such as breast cancer [13] and glioblastoma [14]. However, the role and mechanism of GCSH in prostate adenocarcinoma have not been uncovered. Taken together,

Table 3

The expression correlation of GCSH with its predicted lncRNAs in prostate adenocarcinoma.

lncRNA name	Gene	R-value	P-value
AC114271.1	**GCSH**	**0.285**	**8.98E-11**
GAS5	**GCSH**	**0.261**	**3.04E-09**
CRNDE	**GCSH**	**0.250**	**1.58E-08**
AL391244.1	**GCSH**	**0.246**	**2.72E-08**
MIR762HG	**GCSH**	**0.225**	**3.96E-07**
AC016590.3	**GCSH**	**0.218**	**8.30E-07**
AL355001.2	**GCSH**	**0.214**	**1.37E-06**
DNAJC27-AS1	**GCSH**	**0.196**	**1.04E-05**
SNHG20	**GCSH**	**0.180**	**5.47E-05**
AL117329.1	**GCSH**	**0.174**	**9.57E-05**
SNHG15	**GCSH**	**0.155**	**5.29E-04**
SNHG17	**GCSH**	**0.135**	**2.59E-03**
SSSCA1-AS1	**GCSH**	**0.125**	**5.04E-03**
LINC01521	**GCSH**	**0.120**	**7.16E-03**
AFDN-DT	**GCSH**	**0.101**	**2.34E-02**
AC012640.2	**GCSH**	**0.289**	**5.08E-11**
AC091271.1	**GCSH**	**0.288**	**5.26E-11**
ILF3-AS1	**GCSH**	**0.269**	**1.02E-09**
AL391244.1	**GCSH**	**0.246**	**2.72E-08**
AC092803.2	**GCSH**	**0.244**	**3.26E-08**
AC100810.1	**GCSH**	**0.15**	**7.66E-04**
AL603839.3	**GCSH**	**0.109**	**1.49E-02**
SNHG5	**GCSH**	**0.089**	**4.60E-02**
BX890604.1	GCSH	0.054	2.30E-01
THUMPD3-AS1	GCSH	0.052	2.44E-01
MIR4458HG	GCSH	0.039	3.90E-01
AL121832.3	GCSH	0.035	4.39E-01
AL117379.1	GCSH	0.015	7.36E-01
AL355488.1	GCSH	0.014	7.50E-01
AP000873.2	GCSH	−0.006	9.00E-01
LINC00511	GCSH	−0.034	4.47E-01
AL513327.3	GCSH	−0.089	4.60E-02
HCG18	GCSH	−0.126	4.79E-03
NEAT1	GCSH	−0.142	1.49E-03
PCBP1-AS1	GCSH	−0.159	3.69E-04
VASH1-AS1	GCSH	0.074	9.67E-02
AC008771.1	GCSH	0.071	1.13E-01
AC239868.1	GCSH	0.070	1.16E-01
LPP-AS2	GCSH	0.069	1.22E-01
STARD7-AS1	GCSH	0.036	4.16E-01
AC097103.2	GCSH	0.026	5.63E-01
AL117350.1	GCSH	−0.045	3.16E-01
LINC00893	GCSH	−0.069	1.23E-01
Z97832.2	GCSH	−0.122	6.19E-03
NEAT1	GCSH	−0.142	1.49E-03
SH3BP5-AS1	GCSH	−0.150	7.57E-04
AC005154.1	GCSH	−0.183	4.01E-05

The bold values indicate that these results are statistically significant (Positive correlation).

GCSH might be served as a potential novel therapeutic target and prognostic biomarker in prostate adenocarcinoma.

Protein-protein interaction analysis and enrichment analysis revealed that these genes correlated with GCSH were significantly enriched in several pathways, including TCA cycle. One paper published in *Science* showed that lipoylated TCA cycle proteins were involved in copper-induced cell death cuproptosis [15], indicating that GCSH might interact with other genes by TCA cycle, at least partially.

Leuprolide is a widely-used for treatment of lots of human disorders, such as endometriosis, precocious puberty and prostate cancer [16]. The analytic result revealed that GCSH expression was markedly upregulated in leuprolide-treated response group when compared with non-response group and GCSH possessed the statistical ability to distinguish non-response prostate adenocarcinoma patients from response counterparts who received treatment of leuprolide, which implied that GCSH might be a potential indicator for predicting therapeutic sensitivity of leuprolide in prostate adenocarcinoma.

It has been widely acknowledged that ncRNAs, including miRNA and lncRNA, were widely involved in regulation of gene (including GCSH) expression and function partially *via* sponge mechanism, namely ceRNA hypothesis [17–19]. To ascertain if ceRNA mechanism participates in modulation of GCSH in prostate adenocarcinoma, miRNA prediction, correlation analysis, expression analysis and validation and ROC curve analysis were successively conducted. Consequently, three miRNAs, consisting of miR-212–3p, miR-29a-3p and miR-410–3p, were identified as the potential upstream miRNAs of GCSH in prostate adenocarcinoma. Among the three miRNAs, miR-212–3p and miR-29a-3p acted as tumor suppressors in prostate adenocarcinoma [20–23]. However, miR-410–3p
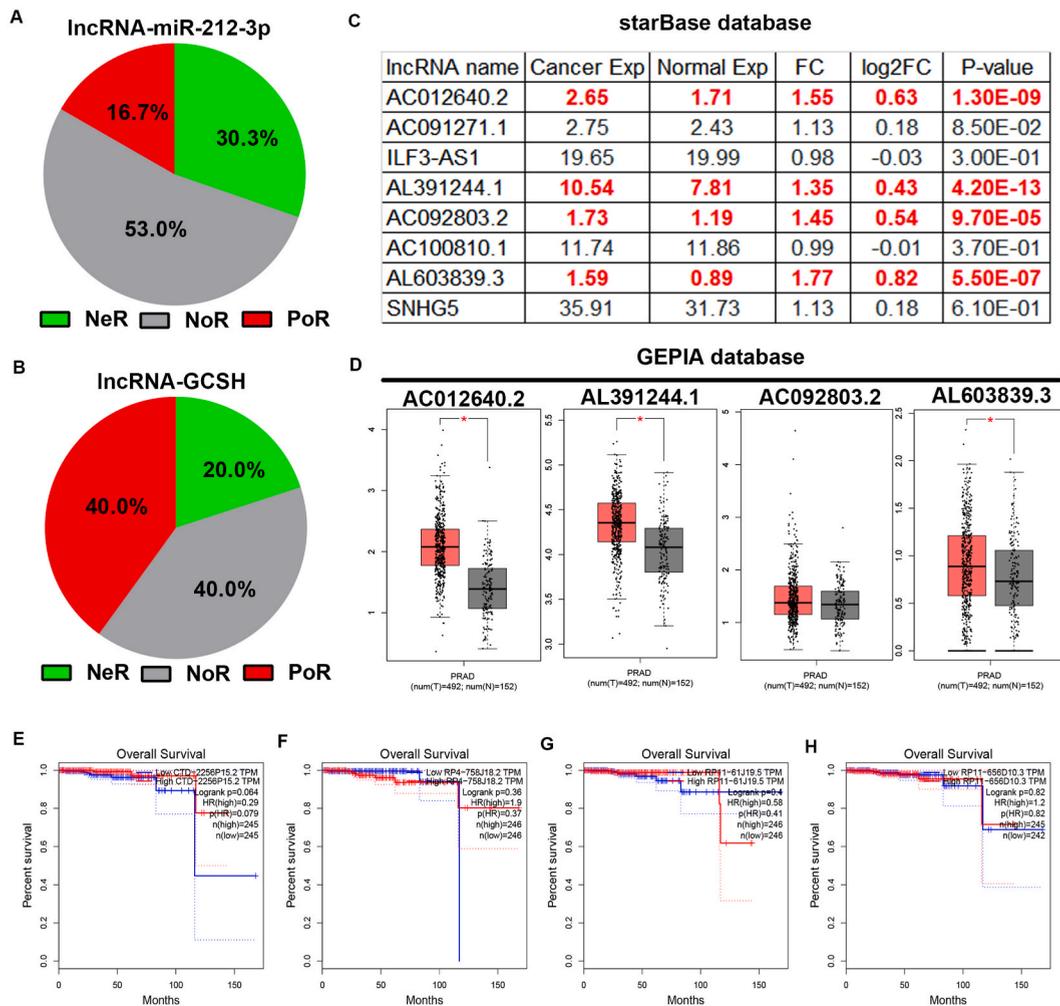
Fig. 6. Prediction and analysis of upstream lncRNAs of miR-212-3p/GCSH in prostate adenocarcinoma. (A) The pie chart of the expression correlation of miR-212–3p with its predicted lncRNAs in prostate adenocarcinoma analyzed by starBase database. (B) The pie chart of the expression correlation of GCSH with the lncRNAs negatively correlated with miR-212–3p in prostate adenocarcinoma analyzed by starBase database. (C) The expression landscape of the potential lncRNAs in prostate adenocarcinoma analyzed by starBase database. (D) The expression levels of upregulated potential lncRNAs in prostate adenocarcinoma validated by GEPIA database. The prognostic values of AC012640.2 (E), AL391244.1 (F), AC092803.2 (G) and AL603839.3 (H) in prostate adenocarcinoma determined by GEPIA database. $*P < 0.05$.

was found to enhance prostate cancer progression by targeting PTEN/AKT/mTOR signaling pathway in prostate cancer [9]. Taken together, miR-212–3p and miR-29a-3p were selected for subsequent analysis.

Next, the upstream lncRNAs of miR-212–3p or miR-29a-3p were predicted. Based on ceRNA mechanism [24], the potential binding lncRNAs should be negatively correlated with miR-212–3p or miR-29a-3p, and should be positively associated with GCSH expression in prostate adenocarcinoma. After performing expression analysis and survival analysis for these predicted lncRNAs in prostate adenocarcinoma, only SNHG17 was identified as the most potential cuproptosis-related lncRNA, which was the upstream lncRNA of miR-29a-3p/GCSH axis. Several studies have documented that SHNG17 functioned as an oncogenic lncRNA in prostate adenocarcinoma. For example, Zhao et al. showed that SNHG17 promoted aggressiveness of prostate cancer cells [25]; Wu et al. suggested that SNHG17 enhanced progression of prostate cancer by modulating its homolog SNORA71B [26]; Bai et al. confirmed that SHNG17 could aggravate proliferation and invasion of castration-resistant prostate cancer [27].

Our analytic results together with these publications implied that SNHG17/miR-29a-3p/GCSH might be a potential cuproptosis-related ceRNA axis in prostate adenocarcinoma, providing key clues for developing effective therapeutic targets and offering strong support to overcome prostate adenocarcinoma. However, these findings should be further validated by much more cell and animal assays and large clinical trials in the future.
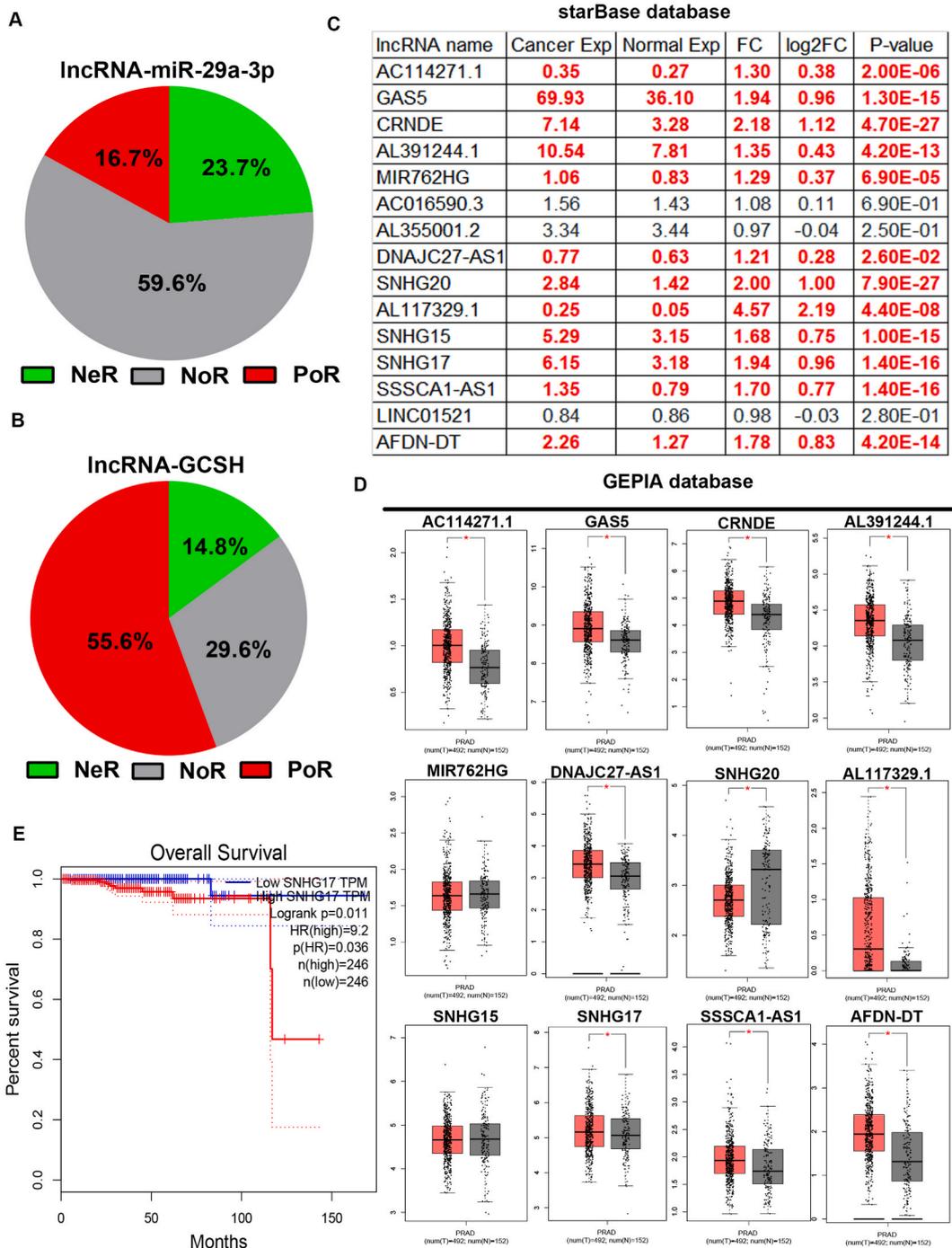
A

lncRNA-miR-29a-3p

16.7%   23.7%

59.6%

☐ NeR ☐ NoR ☐ PoR

B

lncRNA-GCSH

14.8%

55.6%   29.6%

☐ NeR ☐ NoR ☐ PoR

C

starBase database

lncRNA name	Cancer Exp	Normal Exp	FC	log2FC	P-value
AC114271.1	**0.35**	**0.27**	**1.30**	**0.38**	**2.00E-06**
GAS5	**69.93**	**36.10**	**1.94**	**0.96**	**1.30E-15**
CRNDE	**7.14**	**3.28**	**2.18**	**1.12**	**4.70E-27**
AL391244.1	**10.54**	**7.81**	**1.35**	**0.43**	**4.20E-13**
MIR762HG	**1.06**	**0.83**	**1.29**	**0.37**	**6.90E-05**
AC016590.3	1.56	1.43	1.08	0.11	6.90E-01
AL355001.2	3.34	3.44	0.97	-0.04	2.50E-01
DNAJC27-AS1	**0.77**	**0.63**	**1.21**	**0.28**	**2.60E-02**
SNHG20	**2.84**	**1.42**	**2.00**	**1.00**	**7.90E-27**
AL117329.1	**0.25**	**0.05**	**4.57**	**2.19**	**4.40E-08**
SNHG15	**5.29**	**3.15**	**1.68**	**0.75**	**1.00E-15**
SNHG17	**6.15**	**3.18**	**1.94**	**0.96**	**1.40E-16**
SSSCA1-AS1	**1.35**	**0.79**	**1.70**	**0.77**	**1.40E-16**
LINC01521	0.84	0.86	0.98	-0.03	2.80E-01
AFDN-DT	**2.26**	**1.27**	**1.78**	**0.83**	**4.20E-14**

D

GEPIA database

E

Fig. 7. Prediction and analysis of upstream lncRNAs of miR-29a-3p/GCSH in prostate adenocarcinoma. (A) The pie chart of the expression correlation of miR-29a-3p with its predicted lncRNAs in prostate adenocarcinoma analyzed by starBase database. (B) The pie chart of the expression correlation of GCSH with the lncRNAs negatively correlated with miR-29a-3p in prostate adenocarcinoma analyzed by starBase database. (C) The expression landscape of the potential lncRNAs in prostate adenocarcinoma analyzed by starBase database. (D) The expression levels of upregulated potential lncRNAs in prostate adenocarcinoma validated by GEPIA database. (E) The prognostic value of SNHG17 in prostate adenocarcinoma determined by GEPIA database. *$P < 0.05$.
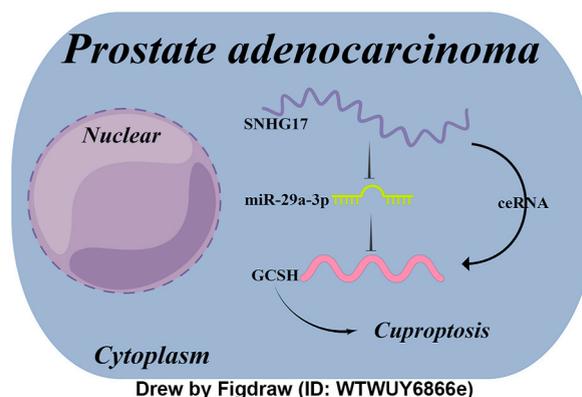
Fig. 8. Establishment of a potential cuproptosis-related SNHG17/miR-29a-3p/GCSH axis in prostate adenocarcinoma.

4. Materials and methods

4.1. starBase analysis

StarBase (http://starBase.sysu.edu.cn/) [28,29] is a database for decoding miRNA-ceRNA, miRNA-ncRNA and RNA-protein interaction networks from CLIP-Seq data, which was employed to determine the expression levels of cuprotosis-related genes, miR-NAs and lncRNAs in prostate adenocarcinoma. P-value<0.05 was considered as statistically significant. The expression correlation of GCSH-miRNA, GCSH-lncRNA as well as miRNA-lncRNA in breast cancer was also assessed by starBase database. P-value<0.05 was considered as statistically significant. Besides, the lncRNAs that could potentially bind to miR-212–3p or miR-29a-3p were predicted and downloaded from starBase database.

4.2. GEPIA analysis

GEPIA (http://gepia.cancer-pku.cn/) [30,31], a developed interactive web server for analyzing the RNA sequencing expression data of more than 9000 tumors and more than 8000 normal samples from the TCGA and GTEx projects, was utilized to validate the expression of cuprotosis-related genes and lncRNAs in prostate adenocarcinoma. P-value<0.05 was considered as statistically significant. Moreover, the prognostic values of potential lncRNAs in prostate adenocarcinoma were also evaluated by GEPIA database. Logrank P-value<0.05 was considered as statistically significant. Additionally, the genes that were significantly correlated with GCSH in prostate adenocarcinoma were also obtained by GEPIA database. Correlation co-efficient>0.3 was included for subsequent analysis.

4.3. UALCAN analysis

UALCAN (http://ualcan.path.uab.edu/index.html) [32,33] is a comprehensive, user-friendly, and interactive web resource for analyzing cancer OMICS data, which was used to detect the prognostic values of cuproptosis-related NFE2L2, ATP7B, CDKN2A, GCSH and DLST in TCGA prostate adenocarcinoma and normal prostate samples. Furthermore, the expression levels of miR-212–3p, miR-29a-3p, miR-410–3p and miR-144–3p in prostate adenocarcinoma were also determined by UALCAN database. P-value<0.05 was considered as statistically significant. The genes that were significantly correlated with GCSH in prostate adenocarcinoma were also acquired by UALCAN database. Correlation co-efficient>0.3 was included for subsequent analysis.

4.4. STRING analysis

STRING (https://cn.string-db.org/cgi/input.pl) [34] is an online database for protein-protein networks and functional characterization of user-uploaded gene/measurement sets, which was used to construct a GCSH-related protein-protein interaction network. The included protein-protein pairs should meet combined score more than 0.4. Besides, GO functional annotation and pathway enrichment analysis for these genes were also conducted using this database. The top five enriched GO terms or pathways were presented with respective false discovery rate.

4.4.1. cBioPortal analysis

cBioPortal (http://cbioportal.org) [35], a widely-used database for comprehensive analysis of complex cancer genomics and clinical profiles, was utilized to acquire the genes that were significantly correlated with GCSH in prostate adenocarcinoma. Correlation co-efficient>0.3 was included for subsequent analysis.

4.5. Venny 2.1.0 analysis

The most potential genes correlated with GCSH in prostate adenocarcinoma were identified by performing intersection analysis for the correlated genes from GEPIA, UALCAN and cBioPortal databases using Venny 2.1.0 (https://bioinfogp.cnb.csic.es/).

4.6. CTR-DB analysis

CTR-DB (http://ctrdb.ncpsb.org.cn/) [36] is a unique tool for basic and clinical researchers to access, integrate and reuse clinical transcriptomes with cancer drug response, which was introduced to analyze the role of GCSH in predicting the therapeutic sensitivity of leuprolide in prostate adenocarcinoma. One dataset (ID: CTR_RNAseq_234) containing 21 samples (6 "leuprolide non-response" samples and 15 "leuprolide response" samples) were finally included for differential analysis and ROC curve analysis.

4.7. TISIDB analysis

TISIDB (http://cis.hku.hk/TISIDB/index.php) [37], an integrated repository portal for tumor-immune system interactions, was employed to predict the potential drugs targeting GCSH. The gene-drug network was downloaded from TISIDB database.

4.8. miRNA prediction

The upstream miRNAs of GCSH were predicted by PITA, RNA22, miRmap, microT, miRanda, PicTar and TargetScan databases. The miRNAs predicted by one of these databases were included for subsequent analysis. The miRNA-GCSH regulatory network was established by Cytoscape software.

4.9. CancerMIRNome analysis

CancerMIRNome (http://bioinfo.jialab-ucr.org/CancerMIRNome) [38] is an interactive analysis and visualization database for miRNome profiles of human cancer, which was introduced to validate the expression of miR-212–3p, miR-29a-3p, miR-410–3p and miR-144–3p and assess their diagnostic values in prostate adenocarcinoma. P-value<0.05 was considered as statistically significant.

4.10. Statistical analysis

All the bioinformatic statistical analyses were automatically calculated by the above online databases or tools. P-value<0.05 was considered as statistically significant.

Funding

Data availability statement

The original contributions presented in the study are included in this article/Supplementary Materials and further inquiries can be directly contacted with corresponding author.

CRediT authorship contribution statement

Shuyuan Xiao: Formal analysis, Investigation, Methodology, Software, Writing – original draft. **Weiyang Lou:** Conceptualization, Funding acquisition, Supervision, Validation, Writing – review & editing.

Declaration of competing interest

The authors declare that they have no known competing financial interests or personal relationships that could have appeared to influence the work reported in this paper.

Acknowledgements

Appendix A. Supplementary data

Supplementary data to this article can be found online at https://doi.org/10.1016/j.heliyon.2023.e21506.

References

[1] C. Parker, E. Castro, K. Fizazi, A. Heidenreich, P. Ost, G. Procopio, et al., Prostate cancer: ESMO Clinical Practice Guidelines for diagnosis, treatment and follow-up, Ann. Oncol. official journal of the European Society for Medical Oncology 31 (9) (2020) 1119–1134.

[2] N. Peng, Z. Zhang, Y. Wang, M. Yang, J. Fan, Q. Wang, et al., Down-regulated LINC00115 inhibits prostate cancer cell proliferation and invasion via targeting miR-212-5p/FZD5/W, nt/β-catenin axis 25 (22) (2021) 10627–10637.

[3] G. Ashok, R. Das, A. Anbarasu, Comprehensive analysis on the diagnostic role of circulatory exosome-based miR-92a-3p for osteoblastic metastases in prostate adenocarcinoma 36 (8) (2023), e3042.

[4] D. Tang, X. Chen, Cuproptosis: a copper-triggered modality of mitochondrial cell death 32 (5) (2022) 417–418.

[5] Y. Wang, L. Zhang, Cuproptosis: a New Form of Programmed Cell Death, 2022.

[6] S.R. Li, L.L. Bu, L. Cai, Cuproptosis: lipoylated TCA cycle proteins-mediated novel cell death pathway 7 (1) (2022) 158.

[7] Z. Bian, R. Fan, A novel cuproptosis-related prognostic gene signature and validation of differential expression in clear cell renal cell carcinoma 13 (5) (2022).

[8] D.V. Swayzer, V. Gerriets, Leuprolide. *StatPearls*. StatPearls publishing copyright © 2023, StatPearls Publishing LLC.: Treasure Island (FL) ineligible companies. Disclosure: Valerie Gerriets declares no relevant financial relationships with ineligible companies (2023).

[9] Y. Zhang, D. Zhang, J. Lv, S. Wang, Q. Zhang, miR-410-3p promotes prostate cancer progression via regulating PTEN/AKT/mTOR signaling pathway, Biochem. Biophys. Res. Commun. 503 (4) (2018) 2459–2465.

[10] W. Lou, B. Ding, G. Zhong, C. Du, W. Fan, P. Fu, Dysregulation of pseudogene/lncRNA-hsa-miR-363-3p-SPOCK2 pathway fuels stage progression of ovarian cancer, Aging 11 (23) (2019) 11416–11439.

[11] J. Zhang, W. Lou, A key mRNA-miRNA-lncRNA competing endogenous RNA triple sub-network linked to diagnosis and prognosis of hepatocellular carcinoma, Front. Oncol. 10 (2020) 340.

[12] H. Zheng, B. Ding, K. Xue, J. Yu, W. Lou, Construction of a lncRNA/pseudogene-hsa-miR-30d-5p-GJA1 regulatory network related to metastasis of pancreatic cancer, Genomics 113 (4) (2021) 1742–1753.

[13] A. Adamus, P. Müller, B. Nissen, A. Kasten, S. Timm, GCSH antisense regulation determines breast cancer cells' viability 8 (1) (2018), 15399.

[14] Ż. Kałuzińska, D.P.L.E.K. Kołat, G.C.S.H. Rrm, A novel WWOX-dependent biomarker triad of glioblastoma at the crossroads of cytoskeleton reorganization and metabolism alterations 13 (12) (2021).

[15] P.A. Cobine, D.C. Brady, Cuproptosis: cellular and molecular mechanisms underlying copper-induced cell death, Mol. Cell 82 (10) (2022) 1786–1787.

[16] D.V. Swayzer, V. Gerriets, Leuprolide. *StatPearls*. StatPearls Publishing Copyright © 2022, StatPearls Publishing LLC, Treasure Island (FL), 2022.

[17] W. Lou, W. Wang, J. Chen, S. Wang, Y. Huang, ncRNAs-mediated high expression of SEMA3F correlates with poor prognosis and tumor immune infiltration of hepatocellular carcinoma, Mol. Ther. Nucleic Acids 24 (2021) 845–855.

[18] W. Lou, J. Chen, B. Ding, W. Fan, XIAP, commonly targeted by tumor suppressive miR-3607-5p and miR-3607-3p, promotes proliferation and inhibits apoptosis in hepatocellular carcinoma, Genomics 113 (3) (2021) 933–945.

[19] W. Lou, B. Ding, G. Zhong, J. Yao, W. Fan, P. Fu, RP11-480I12.5-004 promotes growth and tumorigenesis of breast cancer by relieving miR-29c-3p-mediated AKT3 and CDK6 degradation, Mol. Ther. Nucleic Acids 21 (2020) 916–931.

[20] H.L. Yang, Y.M. Gao, J.A. Zhao, miR-140-5p inhibits human glioma cell growth and invasion by targeting JAG1, Mol. Med. Rep. 16 (3) (2017) 3634–3640.

[21] B. Hu, X. Jin, J. Wang, MicroRNA-212 targets mitogen-activated protein kinase 1 to inhibit proliferation and invasion of prostate cancer cells, Oncology research 26 (7) (2018) 1093–1102.

[22] W. Fu, T. Tao, M. Qi, L. Wang, J. Hu, X. Li, et al., MicroRNA-132/212 upregulation inhibits TGF-β-mediated epithelial-mesenchymal transition of prostate cancer cells by targeting SOX4, Prostate 76 (16) (2016) 1560–1570.

[23] J. Li, X. Wan, W. Qiang, T. Li, W. Huang, S. Huang, et al., MiR-29a suppresses prostate cell proliferation and induces apoptosis via KDM5B protein regulation, Int. J. Clin. Exp. Med. 8 (4) (2015) 5329–5339.

[24] L. Salmena, L. Poliseno, Y. Tay, L. Kats, P.P. Pandolfi, A ceRNA hypothesis: the Rosetta Stone of a hidden RNA language? Cell 146 (3) (2011) 353–358.

[25] H. Zhao, H. Dong, P. Wang, H. Zhu, Long non-coding RNA SNHG17 enhances the aggressiveness of C4-2 human prostate cancer cells in association with β-catenin signaling, Oncol. Lett. 21 (6) (2021) 472.

[26] G. Wu, C. Hao, X. Qi, J. Nie, W. Zhou, J. Huang, et al., LncRNA SNHG17 aggravated prostate cancer progression through regulating its homolog SNORA71B via a positive feedback loop, Cell Death Dis. 11 (5) (2020) 393.

[27] M. Bai, Y. Lei, M. Wang, J. Ma, P. Yang, X. Mou, et al., Long non-coding RNA SNHG17 promotes cell proliferation and invasion in castration-resistant prostate cancer by targeting the miR-144/CD51 Axis, Front. Genet. 11 (2020) 274.

[28] J.H. Li, S. Liu, H. Zhou, L.H. Qu, J.H. Yang, starBase v2.0: decoding miRNA-ceRNA, miRNA-ncRNA and protein-RNA interaction networks from large-scale CLIP-Seq data, Nucleic Acids Res. 42 (Database issue) (2014) D92–D97.

[29] J.H. Yang, J.H. Li, P. Shao, H. Zhou, Y.Q. Chen, L.H. Qu, starBase: a database for exploring microRNA-mRNA interaction maps from Argonaute CLIP-Seq and Degradome-Seq data, Nucleic Acids Res. 39 (Database issue) (2011) D202–D209.

[30] C. Li, Z. Tang, W. Zhang, Z. Ye, F. Liu, GEPIA2021: integrating multiple deconvolution-based analysis into GEPIA 49 (W1) (2021) W242–w246.

[31] Z. Tang, C. Li, B. Kang, G. Gao, C. Li, Z. Zhang, GEPIA: a web server for cancer and normal gene expression profiling and interactive analyses, Nucleic Acids Res. 45 (W1) (2017) W98–w102.

[32] D.S. Chandrashekar, B. Bashel, S.A.H. Balasubramanya, C.J. Creighton, I. Ponce-Rodriguez, B. Chakravarthi, et al., UALCAN: a portal for facilitating tumor subgroup gene expression and survival analyses, Neoplasia 19 (8) (2017) 649–658.

[33] D.S. Chandrashekar, S.K. Karthikeyan, P.K. Korla, H. Patel, A.R. Shovon, M. Athar, et al., UALCAN: an update to the integrated cancer data analysis platform, Neoplasia 25 (2022) 18–27.

[34] D. Szklarczyk, A.L. Gable, K.C. Nastou, D. Lyon, R. Kirsch, S. Pyysalo, et al., The STRING database in 2021: customizable protein-protein networks, and functional characterization of user-uploaded gene/measurement sets, Nucleic Acids Res. 49 (D1) (2021) D605–d612.

[35] J. Gao, B.A. Aksoy, U. Dogrusoz, G. Dresdner, B. Gross, S.O. Sumer, et al., Integrative analysis of complex cancer genomics and clinical profiles using the cBioPortal, Sci. Signal. 6 (269) (2013) pl1.

[36] Z. Liu, J. Liu, X. Liu, CTR-DB, an omnibus for patient-derived gene expression signatures correlated with cancer drug response 50 (D1) (2022) D1184–d1199.

[37] B. Ru, C.N. Wong, Y. Tong, J.Y. Zhong, S.S.W. Zhong, W.C. Wu, et al., TISIDB: an integrated repository portal for tumor-immune system interactions, Bioinformatics 35 (20) (2019) 4200–4202.

[38] R. Li, H. Qu, S. Wang, CancerMIRNome: an interactive analysis and visualization database for miRNome profiles of human cancer 50 (D1) (2022) D1139–d1146.